Determination of the point and space groups for hydroxyapatite by computer simulation of CBED electron diffraction patterns

E. Sánchez-Pastenes[a] and J. Reyes-Gasga[b]
Instituto de Física, UNAM,
Apdo. Postal 20-364, 01000 México, D.F., México,
e-mail: [a]elson@fisica.unam.mx, [b]jreyes@fisica.unam.mx

Recibido el 20 de enero de 2005; aceptado el 30 de agosto de 2005

The structure of natural hydroxyapatite nHAP (*i.e.* the hydroxyapatite found in teeth and bones) has not been completely characterized experimentally until now. This involves the study of the structural characteristics of synthetic hydroxyapatite sHAP (*i.e.* one whose stoichiometric formula is Ca_{10} $(PO_4)_6$ $(OH)_2$) using many techniques, in particular electron diffraction computer simulation. Thus, any variation presented in its structure will be easily detected. In this work we comment on the crystallographic elements presented in simulated convergent beam electron diffraction (CBED) patterns for sHAP, in its versions of Laue Zones of Zero Order (ZOLZ), First Order (FOLZ), Second Order (SOLZ) and Higher Order (HOLZ), and the deduction of its space group $P6_3/m$. These results are compared with those reported experimentally.

Keywords: CBED; hydroxyapatite; electron diffraction.

Experimentalmente se ha observado que la estructura de la hidroxiapatita natural nHAP (*i.e.* el componente inorgánico mayoritario de los dientes y los huesos) no ha sido completamente caracterizada hasta el momento. Esto nos lleva a estudiar las características estructurales y cristalográficas de la hidroxiapatita sintética sHAP (i.e. aquella que obedece la estequiometría de la fórmula Ca_{10} $(PO_4)_6$ $(OH)_2$) por medio de diferentes técnicas, en particular la simulación computacional de los patrones de difracción electrónica, para contar con una base sólida que nos permita compararlas. En este trabajo se comentan los elementos de simetría que se observan en los patrones simulados computacionalmente de haz convergente (CBED) para sHAP, en sus versiones de zonas de Laue de orden cero (ZOLZ), de primer orden (FOLZ), de segundo orden (SOLZ) y de orden mayor (HOLZ), y se deduce su grupo espacial $P6_3/m$ a partir de éstos. Los resultados obtenidos se comparan con los reportados experimentalmente para nHAP.

Descriptores: CBED; hidroxiapatita; difracción electrónica.

PACS: 61.14.-x

1. Introduction

To define the symmetry (point group and space group) in crystals is an indispensable step prior to resolving the crystal structure. This study can start with X-ray diffraction analysis for determining the unit cell dimensions in an approach to obtaining the space group. However, when the technique of convergent beam electron diffraction (CBED) is used, we can easily determine the symmetry of crystals [1]. In the X-ray technique, the kinematical diffraction theory is applicable, and we cannot determine whether a crystal is polar or non-polar unless the anomalous dispersion effect is included. As a result, the X-ray diffraction method can only identify 11 Laue groups of the 32 points groups [2]. With CBED, however, which is fully based on the dynamical signal of electron diffraction, we are able to distinguish polar crystals from non-polar crystals, and thus achieve the unique identification of point groups. Furthermore, the CBED technique enables us to ascertain the presence of screw axes and glide planes. Therefore, CBED is a very useful technique in determining crystal point-groups and space-groups of materials.

The CBED technique produces electron diffraction patterns using a conical electron beam with an angle of approximately 10^{-3} rad on a uniform and non-bending specimen area of about 10 nm in diameter. Instead of the usual diffraction spots, diffraction disks are produced. All point groups can be determined uniquely by inspecting the symmetries appearing in these disks. Screw axes and glide planes are identified through the analysis of the dynamical diffraction effect: when a crystal has a screw axis or a glide plane, special extinction lines appear in the disks. These lines are named "dynamic extinction lines" or GM lines [1]. By examining whether GM lines are formed or not, most space groups can be identified.

It has been observed that natural hydroxyapatite (nHAP) (*i.e.* hydroxyapatite that makes up teeth and bones for example [3]), presents a structure that is not yet completely characterized [4,5]. Recently, experimental electron diffraction analysis has shown both P6/m and $P6_3/m$ as possible space groups for nHAP [6,7], and the presence of forbidden reflections along the c*-axis in the selected area electron diffraction patterns (SADP) [5]. We have experimentally attempted to carry out the structural analysis of nHAP (in this case, HAP from human tooth enamel) by CBED in otfrt yo study these forbidden reflections [5,6,7], but a completed satisfactory interpretation has not yet been possible. Therefore, in the present work we calculate and comment on the main crystallography characteristics of computer calculated CBED patterns for sHAP in order to use them as a starting point for the theoretical and experimental characterization of nHAP.

2. Simulation procedure

Starting with the data from Brés *et al.* [4] for the atomic positions of Ca, P, O and H in the sHAP unit cell, its adjustment was done with the Rietveld method [8] with R – WP = 9.85% with the data from Young *et al.* [9,10] in otder to ensure the best structural data in our simulation analysis. The resulting data were captured in a INDY Silicon Graphics workstation with the program EMS [11], using the sub-programs "fc4", "hl3", "kp3"and "cb1", and changing the camera length and number of iterations. It is worth mentioning that the average time needed obtain the simulations of CBED patterns in the Zero Order Laue Zone (ZOLZ), First Order Laue Zone (FOLZ) and Higher Order Laue Zone (HOLZ) along different zone axes and crystal thicknesses was from 5 to 13 hours on the average.

To obtain the nHAP samples (in this case, human tooth enamel), we follow the experimental procedure indicated in Ref. 5. The samples had a circular shape with dimensions 0.3 mm in diameter and 100 nm thick. Analytical electron microscopy and the experimental CBED electron patterns were performed using the Jeol 100 CX and Jeol 2010 transmission electron microscopes [see also Refs. 6,7].

3. Results

Figure 1 shows the simulated CBED patterns in ZOLZ for the main directions of the sHAP unit cell. Figure 1a shows a unique 6-fold axis symmetry parallel to$[0001]$, which indicates the point group 6. In Fig. 1b and 1c, there are two mirrors, which indicates a 2mm symmetry along both the $[1\bar{1}20]$

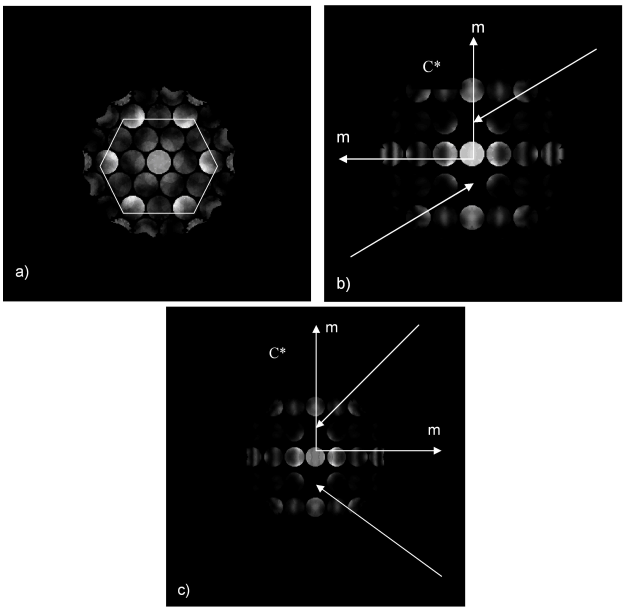

FIGURE 1. Simulated CBED patterns in ZOLZ for sHAP along (a) $[0001]$, (b) $[1\bar{1}20]$, and (c) $[10\bar{1}0]$. Note the mirror symmetry and absence or the reflections 0001 (1odd)in these patterns (indicated by arrows). The sample was 130 nm in thickness.

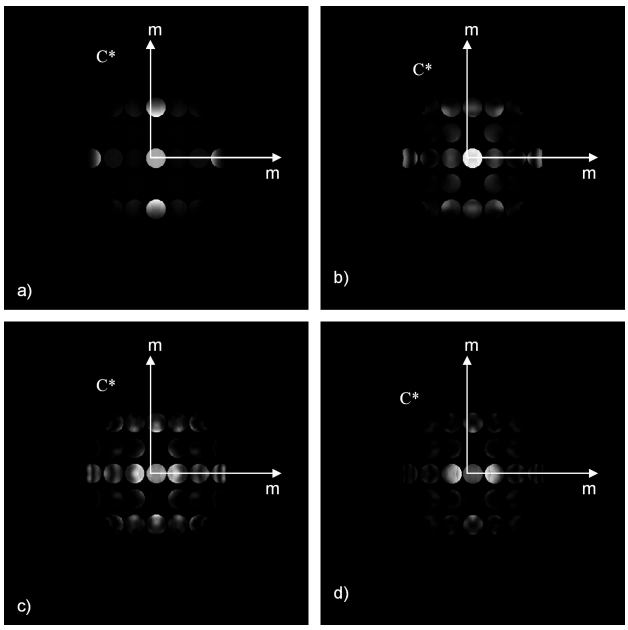

FIGURE 2. Simulated CBED patterns for sHAP with different thicknesses along $[1\bar{1}20]$. Note the peresence of dynamic lines and the absence of forbidden reflections along the c*-axis in each case. a) 10 nm, b) 60 nm, c) 130 nm, d) 150 nm. L=250 mm V=200 kV.

and $[10\bar{1}0]$ directions. Note the absence of the reflections $(000l)$, with l = 2n + 1, in this figure.

Figure 2 shows once again the simulated CBED patterns in ZOLZ along the $[1\bar{1}20]$ direction, but in this case for different thicknesses. Note in this figure that the disks do not present any features from dynamic contrast at 10 nm in thickness, not until the sample reaches a thickness of 60 nm. Also, it is worth noting the absence of the forbidden reflections along the c*-axis (*i.e.* the $(000l)$ reflections, with l = 2n + 1), as the $P6_3/m$ space group suggests, and the existence of two perpendicular mirrors in these patterns.

In Fig. 3 the CBED patterns are observed in ZOLZ and HOLZ. Note in this figure that both ZOLZ and FOLZ present a 6-fold symmetry axis along $[0001]$, while along $[1\bar{1}20]$ and $[10\bar{1}0]$ ZOLZ has two mirrors but FOLZ and SOLZ present only one. That is, the horizontal mirror plane is the same for ZOLZ, FOLZ and SOLZ, and the vertical mirror plane disappears in FOLZ and SOLZ. Therefore, ZOLZ presents symmetry 2mm while FOLZ and SOLZ are only 2m in this figure.

Figure 4 shows the CBED pattern in ZOLZ showing the HOLZ lines generated in the central disk. In Fig. 4a, the pattern shows a 6-fold symmetry axis with two mirrors, which indicates the 6mm symmetry for the central disk along the $[0001]$ direction. In Fig. 4b, and taking into account the relative line intensity, the central disk shows a mirror plane only. A similar situation is shown in Fig. 4c. Therefore, the symmetry observed in the ZOLZ central disk along $[10\bar{1}0]$ and $[1\bar{1}20]$ is "m".

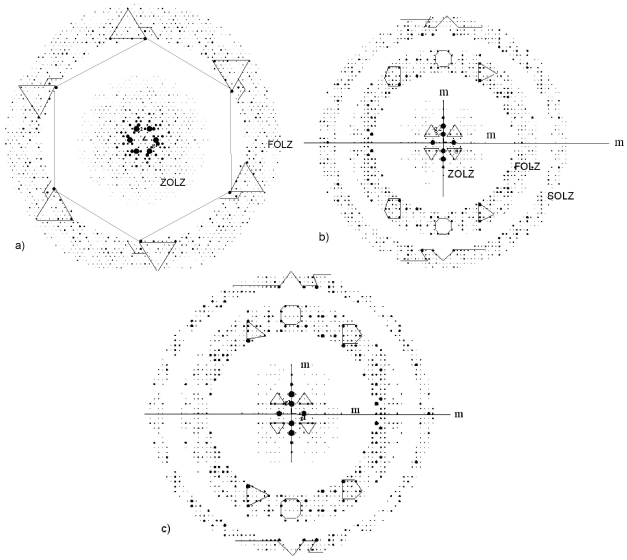

FIGURE 3. Simulated CBED patterns for sHAP in ZOLZ and HOLZ. L = 500 mm. V = 200 kV. a) $[0001]$, b) $\left[10\bar{1}0\right]$, and c) $\left[1\bar{1}20\right]$. Note the disappearance of the mirror plane for HOLZ in (b) and (c). The added geometries are for clarity of the symmetry elements only.

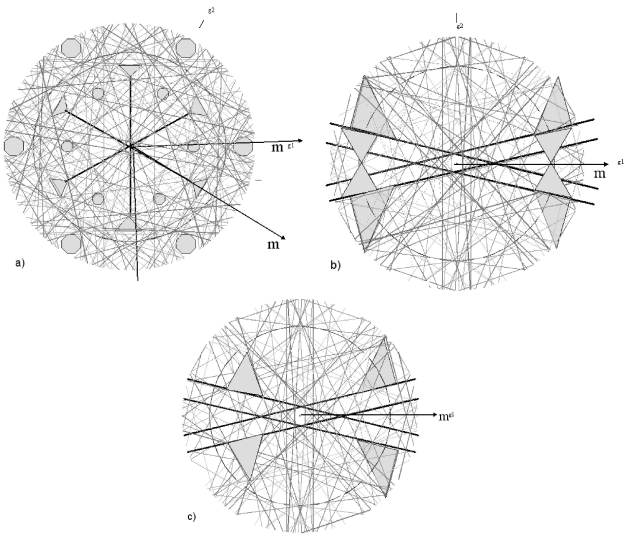

FIGURE 4. Simulated CBED central disk patterns for sHAP in ZOLZ. a) $[0001]$, b) $\left[10\bar{1}0\right]$, and c) $\left[1\bar{1}20\right]$. L= 17.8 m, V=100 kV. Note the existence of mirror planes "m" in the central disks.

For comparing these simulated CBED patterns with those of nHAP experimentally obtained from human tooth enamel [4-7], Fig. 5 is included. Figures 5a (experimental) and 5b (simulated) show the CBED pattern in ZOLZ along the $[0001]$ direction; both patterns show the symmetry 6. Figures 5c (experimental) and 5d (simulated) show the ZOLZ pattern along the $\left[1\bar{1}20\right]$ direction; in both cases, the absence of the forbidden reflections is observed, although the dynamic lines were not registered in 5c because of experimental conditions [4,6]. In Figs. 5e (experimental) and 5f (simulated), Kikuchi lines in FOLZ and ZOLZ are shown. We observe, therefore, in Fig. 5 that the experimental and

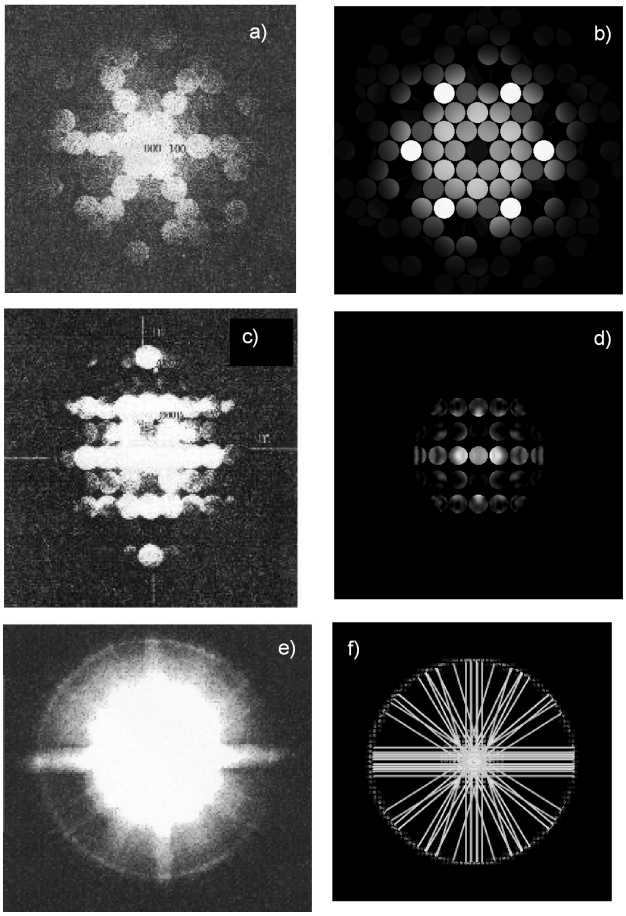

FIGURE 5. Experimental (a,c,e) and simulated (b,d,f) CBED patterns for sHAP. a) and b) $[0001]$ CBED in ZOLZ, c) and d) $\left[1\bar{1}20\right]$, e) and f) Kikuchi lines pattern with CBED in ZOLZ and FOLZ along $\left[1\bar{1}20\right]$ direction. Note the similarity of these patterns.

simulated CBED patterns for HAP show very good similarities. Unfortunately, the experimental CBED patterns are not as good in quality because of experimental conditions [4-6,9,10], and we are unable to make a better comparison.

4. Discussion

With the above results, using Table I, wich shows the relationship among the symmetries observed in the CBED patterns and the point groups for the hexagonal system, we find the possible point group for sHAP [1,9]. We observe that ZOLZ indicates the symmetry 2mm (Figs. 1b and 1c), generating the projection diffraction group $2mm1_R$, while the 6-fold symmetry produces the projection diffraction group 61_R (Fig. 1a). CBED patterns in FOLZ and SOLZ indicate the 6-fold (Fig. 3a) and "m" (Figs. 3b and 3c) symmetries, while the central disk indicates the 6 mm (fig. 4a) and "m" (Figs. 4b and 4c) symmetries. Therefore, the possible projection diffraction groups are 2 $mm1_R$ for both the $\left[10\bar{1}0\right]$ and $\left[1\bar{1}20\right]$ directions, and 61_R for $[0001]$. This indicates that sHAP shows group 6/m in the $[0001]$ direction and the

TABLE I. Diffraction patterns and corresponding point-groups for a hexagonal system. In bold, the most probable diffraction groups and point groups for sHAP are enhanced

Zone axis	Symmetry in ZOLZ	Projection diffraction group	Diffraction groups	Possible point groups
[0001]	6	61_R	6	6
			6_R	-3, m3
			61_R	**6/m**
$[1\bar{1}20]$	2mm	$2mm1_R$	$2m_Rm_R$	222,422,42m,622,23,432
			2mm	mm2,6m2
			2_Rmm_R 2/m,mmm,4/m,4/mmm,	
			$2mm1_R$	**-3m,6/m,6/mmm,m3,m3m**
				mmm,4/mmm,6/mmm,m3,m3m
$[10\bar{1}0]$	2mm	$2mm1_R$	$2m_Rm_R$	222,422,42m,622,23,432
			2mm	mm2,6m2
			2_Rmm_R2/m,mmm,4/m,4/mmm,-	
			$2mm1_R$	**3m,6/m,6/mmm,m3,m3m**
				mmm,4/mmm,6/mmm,m3,m3m

TABLE II. Source of the dynamic extinctions in the order zero reflections of CBED patterns for hexagonal structures. In bold, the most probable element of symmetry for sHAP is enhanced.

Unique line of the layer-zero of extinction.	Perpendicular line of the layer-zero of extinction.	Elements of Symmetry
m_R	$2m_Rm_R$	Parallel screw axis to each line of extinction
$2m_Rm_R$	$4m_Rm_R$	
m	2mm	Glide planes parallel to the axis zone and each line of extinction.
2m	4mm	
2_Rmm_R	4_Rmm_R	Glide: if parallel to complete mirror plane
		Screw: if perpendicular to the complete mirror plane
	2_Rmm_R	Parallel glide and perpendicular screw at complete mirror plane.
$m1_R$	$2mm1_R$	**Glide plane and screw axis parallel a each extinction line**..
$2mm1_R$	$4mm1_R$	

groups 6/m and 6/mm in the $[1\bar{1}20]$ and $[10\bar{1}0]$ directions, respectively. Therefore, the most probable point group is 6/m.

We know that the sHAP unit cell is hexagonal primitive. This indicates the P6/m as a space group. Therefore, to unambiguously determine the space group, it is necessary to analyze the formation of dynamic lines in the CBED patterns, which are shown in Fig. 2. For this we use Table II, which indicates the symmetry elements that produce these lines according with the diffraction group obtained in Table I (*i.e.* $2mm1_R$). The absences along the $[10\bar{1}0]$ and $[1\bar{1}20]$ directions correspond to the reflections $00l$ (l odd), which indicates a screw axis 2_1 along the c-axis contained in the symmetry 6_3. Therefore, the space group of sHAP is $P6_3/m$.

Now we know the main characteristics and elements of symmetry of the CBED patterns for sHAP. With these results in mind, we are now in a position to elucidate the origin of any additional crystallographic element that nHAP could present in its electron diffraction patterns, both in SADP and CBED. For example, the experimental observation of forbidden reflections in SADP patterns of human tooth enamel [5] was reported some time ago. These reflections belong to the family $(000l)$ with l = 2n + 1, which are not allowed by the space group $P6_3/m$. Some attempts to explain these observations have been reported, both from the experimental [5-7] and theoretical point of view [9,12]. However, all efforts have fallen short, because of the experimental limits of the equipment used [5-7].

Reyes-Gasga and García-García [12] have calculated the ballistic damages produced by the electron beam of different electron microscopes in sHAP samples; from this calculation it was found that the OH ions are weakly bonded and easily displaced. Thus, the electron beam energy used for the observation of nHAP samples with electron microscopes is

enough for to produce a breakdown of the original structure in HAP crystal, the screw axis mainly.

All these results together must be taken into account for the crystallographic structural characterization of nHAP from the experimental and theoretical points of view.

5. Conclusions

From the simulated patterns for sHAP shown in this work, it is concluded that the CBED patterns present the symmetries 6mm and "m" in the central disk, 6-fold and 2mm in ZOLZ, and 6-fold and "m" in HOLZ. The hexagonal unit cell presents the 6/m point group and $P6_3/m$ space group. The non-existence of the reflections $00l$ (l odd) is characteristic of the $P6_3/m$ space group. Therefore, the experimental observation of these reflections in nHAP [5,9,10] indicates the breakdown in symmetry because of some chemical element substitutions, as reported elsewhere. Unfortunately, its experimental analysis remains a great experimental challenge.

Acknowledgments

We thank M. Aguilar Franco, P. Mexía Hernández, C. Flores Morales, L. Rendón Vázquez, R. Hernández, S. Tehuacanero, C. Zorrilla, J. Cañetas, C. Magaña, and A. Sánchez for their technical help. This work was sponsored by DGAPAUNAM (Project IN-104902)

1. M. Tanaka and M. Terauchi *Convergent-Beam Electron Diffraction* (JEOL LTD, Japan, 1985).
2. J.C. Spence and J.M. Zuo *Electron microdiffraction* (Plenum Press, N.Y. and London, 1992).
3. R.Z. Le Geros *Calcium Phosphates in Oral Biology and Medicine* (Howard M. Myers, Sn. Francisco Cal., 1991).
4. E.F. Brés, P. Steuer, and J.C. Voegel *J. Microscopy* **170** (1993) 147.
5. J. Reyes-Gasga, M. Reyes-Reyes, and R. García, *Mat. Res. Soc. Proc.* **599** (2000) 91.
6. M. Reyes-Reyes, *Estudio cristalográfico del esmalte dental humano por microscopía electrónica, difracción electrónica y de haz convergente.* M. Sc. Thesis on Materials Science UNAM (Mexico 2000).
7. M. Reyes-Reyes, J. Reyes-Gasga, and R. García. *Tip. Revista Especializada en Ciencias Químicas-Biológica* **4** (2001) 40.
8. R.A. Young *The Rietveld Method* (Oxford University Press, 1993).
9. E. Sánchez-Pastenes, *Simulación de los patrones de difracción electrónica de haz convergente de la hidroxiapatita.* M. Sc. Thesis on Materials Science UNAM (Mexico 2001).
10. E. Sánchez-Pastenes and J. Reyes-Gasga, *Latinamerican J. Metall. Mater.* **21** (2001) 69.
11. Software *EMS-Online* http://cecm.insa-lyon.fr/CIOLS/.
12. J. Reyes-Gasga and R. García-García, *Rad. Phys. Chem.* **64** (2002) 359.